INSTITUTE OF PLASMA PHYSICS

NAGOYA UNIVERSITY

SLOW WAVE ANTENNA COUPLING TO ION BERNSTEIN WAVES FOR PLASMA HEATiNG IN ICRF

W.N-C. SY, T. AMANO, R. ANDO, A. FUKUYAMA, T. WATARI

(Received – Oct. 16, 1984)

IPPJ- 702 Oct. 1984

RESEARCH REPORT

NAGOYA, JAPAN

SLOW WAVE ANTENNA COUPLING TO ION BERNSTEIN WAVES FOR PLASMA HEATING IN ICRF

W.N-C. SY*, T. AMANO, R. ANDO, A. FUKUYAMA**,
T. WATARI

(Received - Oct. 16, 1984)

IPPJ - 702 Oct. 1984

Further communication about this report is to be sent to the Research Information Center, Institute of Plasma Physics, Nagoya University, Nagoya 464, Japan.

---

* Research School of Physical Sciences, The Australian National University, Canberra, Australia.
** School of Engineering, Okayama University, Okayama, Japan

ABSTRACT

The coupling of ICRF power from a slow wave antenna to a plasma with finite temperature is examined theoretically and compared to an independent computer calculation. It is shown that such antennas can be highly efficient in transferring most of the antenna power directly to ion Bernstein waves, with only a very small fraction going into fast waves. The potentiality of this coupling scheme for plasma heating in ICRF is briefly discussed.

1. INTRODUCTION

One of the most effective methods for plasma heating in controlled fusion research is to couple RF power into plasma waves at the ion cyclotron range of frequencies (ICRF). Fast waves launched by an external antenna can transfer energy to ion Bernstein waves by mode conversion processes at an ion-ion hybrid layer or at a second harmonic layer [1,2]. Such excitation of ion Bernstein waves and their subsequent absorption by the plasma are considered the essential physical processes occurring in tokamak plasma heating experiments [3-5], where encouraging results of efficient plasma heating have been obtained. However, entirely new ways of launching ion Bernstein waves have been proposed [6,7] and their different merits and demerits have been discussed. Recently, in the ACT-1 plasma, ion Bernstein waves have been launched directly by an electrostatic antenna and efficient ion heating has been achieved [8]. The purpose of the present paper is to assess theoretically, the efficiency of a slow wave antenna in launching ion Bernstein waves.

Successful plasma heating experiments have been carried out first on the RFC-XX device [9] and then more recently on the NBT bumpy torus [10] and the JIPP T-IIU tokamak [11] using the so-called Nagoya type III antenna. This antenna is essentially a slow wave antenna, since its RF current, being aligned along the magnetic field, is expected to excite mainly slow waves e.g., electron plasma waves in a low density plasma. Although the experiments indicate ion Bernstein wave heating is probably involved, there has been no independent verification from experimental measurements or theoretical modelling. Since, for typical parameters, fast waves as well as slow waves could be excited, it is not clear how much of the plasma heating could be attributed to ion Bernstein waves. In this

paper, a model antenna-plasma coupling problem is solved to answer questions concerning energy partition into the various waves. To do this, we take into account explicitly, and apparently for the first time, the three different types of waves: ion Bernstein waves, fast waves and slow waves.

In the next section, a system of basic equations, which is suitable for antenna coupling studies is derived from kinetic theory and the dispersive properties of plasma waves are discussed for a model which simulates the JIPP T-IIU tokamak plasma [11]. To assess the inherent coupling characteristics of a slow wave antenna, a single pass antenna-plasma coupling problem is formulated and solved analytically for a simple model in section 3. Energy fluxes, antenna impedance and partition of wave power are discussed in detail and illustrated numerically in section 4. In the final section, a summary and physical interpretation of the results obtained are presented and the implications for ICRF heating are discussed.

2. BASIC EQUATIONS AND WAVE DISPERSION

The description of ion Bernstein waves requires the inclusion of finite temperature effects whilst the consideration of fast waves should incorporate spatial gradient effects, since their wavelengths at ICRF in present day laboratory plasmas are comparable to scalelengths of nonuniformities. A general theory of plasma waves which includes both finite temperature effects and spatial gradients effects is well known to be rather complicated [12-14]. In this section, a system of differential equations which is sufficient to model the antenna-plasma coupling problems considered in this paper is derived from kinetic theory.

In SI units, the Maxwell's equations when Fourier transformed in time read

$$\nabla \cdot \vec{E} = i\omega\vec{B}, \quad \nabla \times \vec{B} = -i\omega\vec{E}/c^2 + \mu_0\vec{j},$$

where $\vec{j}$ is the induced current density. The main problem is to relate $\vec{j}$ to the electromagnetic field, taking into account the appropriate plasma properties and responses. A local linear approximation gives

$$\vec{j} = \overleftrightarrow{\sigma}(\omega,\nabla).\vec{E},$$

where the conductivity tensor $\overleftrightarrow{\sigma}$ contains both finite temperature effects and spatial derivatives designated by ∇. For a plasma with inhomogeneity in the x direction, perpendicular to the magnetic field $\vec{B}_0$, an expansion in terms of the ratio of the Larmor radius to the scalelengths of nonuniformity gives [13,14]

$$\overleftrightarrow{\sigma} \approx i\omega\varepsilon_0 \left\{ \overleftrightarrow{\chi}_0 + \overleftrightarrow{\chi}_1 \frac{c}{\omega}\frac{d}{dx} + \overleftrightarrow{\chi}_2 \frac{c^2}{\omega^2}\frac{d^2}{dx^2} + \cdots \right\},$$

where $\overleftrightarrow{\chi}_n$ is the susceptibility tensor of n-th order in the Larmor radius. Introduction of the dielectric tensor $\overleftrightarrow{K}$ by

$$\overleftrightarrow{K} \equiv \overleftrightarrow{I} + i\overleftrightarrow{\sigma}/\omega\varepsilon_0 ,$$

allows Maxwell's equations to be written as

$$\nabla \times \vec{E} = i\omega\vec{B}, \quad \nabla \times \vec{B} = -(i\omega/c^2)\overleftrightarrow{K}.\vec{E} . \qquad (1), (2)$$

To address the particular questions on antenna-plasma coupling, dissipation and hence collisions and wave-particle interactions may be neglected. It can be shown from the Vlasov equation that in a finite Larmor radius expansion of the dielectric tensor:

$$\overleftrightarrow{K} = \overleftrightarrow{K}_0 + \overleftrightarrow{K}_1 + \overleftrightarrow{K}_2 + \ldots ,$$

$\overleftrightarrow{K}_0$ is the cold plasma dielectric tensor, $\overleftrightarrow{K}_1 = 0$, and $\overleftrightarrow{K}_2 \propto d^2/dx^2$, with $\vec{B}_0.\overleftrightarrow{K}_2 = \overleftrightarrow{K}_2.\vec{B}_0 = 0$. Ordering considerations and comparisons of *sizes of various terms show that a suitable dielectric tensor* $\overleftrightarrow{K}$ *can* be defined by

$$\overleftrightarrow{K} \equiv \begin{pmatrix} S + \tau\partial_x^2 & -iD & . \\ iD & S & . \\ . & . & P \end{pmatrix} , \qquad (3)$$

where S, D and P are defined in Stix's notation [15] and the term arising from finite temperature modifications is given by

$$\tau \equiv \sum_i 3\omega_{pi}^2 T_i/m_i(\omega^2-4\Omega_i^2)(\omega^2-\Omega_i^2) \ .$$

In this expression, ω_{pi}, Ω_i, T_i, m_i are respectively the plasma frequency, gyrofrequency, temperature and mass of the particles, and summation need only be carried over the ions, since finite Larmor radius effects due to the electrons are negligible by comparison.

In a one dimensional model without magnetic shear (see fig. 1), spatial Fourier transform may be carried out in the y and z directions. Since the y variation is not essential to an understanding of the antenna coupling problem, we set $k_y = 0$ for simplicity. On introducing dimensionless variables,

$$\xi = x\omega/c \ , \qquad T \equiv -\tau\omega^2/c^2 \ ,$$

it follows from equation (1)-(3), a system of basic equations may be written as

$$iT\frac{d^2E_x}{d\xi^2} - i(S-n_z^2)E_x - DE_y = n_z\frac{dE_z}{d\xi} \ , \tag{4}$$

$$\frac{d^2E_y}{d\xi^2} + iDE_x + (S-n_z^2)E_y = 0 \ , \tag{5}$$

$$\frac{d^2E_z}{d\xi^2} + PE_z = in_z\frac{dE_x}{d\xi} \ , \tag{6}$$

where $n_z \equiv k_z c/\omega$. This sixth order system of equations describes ion Bernstein waves, fast waves, slow waves and their mutual coupling.

Useful insights can be gained from a dispersion analysis of this system of equations, for which the dispersion relation in n_x^2 reads

$$Tn_x^6 + An_x^4 - Bn_x^2 + C = 0 \ ,$$

where

$$A \equiv S - T(S+P-n_z^2) \ ,$$

$$B \equiv (S-n_z^2)(S+P-TP) - D^2 \ ,$$

$$C \equiv P\{(S-n_z^2)^2 - D^2\} \ .$$

This cubic dispersion equation has been solved numerically for parabolic density profiles and squared parabolic temperature profiles for typical parameters of JIPP T-IIU experiments [11]. From Fig. 1, it is seen that for reasonable estimates of the edge density ($\gtrsim 10^{10}\,cm^{-3}$), the dispersion curves are well separated, indicating the absence of any complicating mode coupling dispersive structure further into the plasma. The short and long wavelength propagating branches represent respectively ion Bernstein waves and fast waves, whilst the evanescent branch represents the slow waves. The dispersion curve for the ion Bernstein waves is in agreement with an independent calculation [11] using a fully kinetic model, but in the electrostatic approximation. This vindicates the small Larmor radius expansion used in deriving the system of basic equations. From an analysis of the ion Bernstein dispersion curves, it is interesting to note that the FLR parameter λ is independent of temperature,

$$\lambda = \frac{1}{3}\,(4-\omega^2/\Omega_i^2) \ .$$

That is, the small Larmor radius expansion is valid even at arbitrarily high temperatures, provided the frequency is sufficiently near the second harmonic ion cyclotron frequency. Finally, it should be mentioned that even though the slow waves are evanescent and do not carry any power well into the plasma, they are nevertheless important in the antenna-plasma coupling calculation, because the parallel electric field E_z is large at the plasma boundary and equation (4) apparently indicates its spatial decay driving the E_x field of the ion Bernstein waves.

3. ANTENNA-PLASMA COUPLING

In order to assess the inherent capability of an antenna to launch the different types of waves in question, it is necessary to solve a single pass problem without dissipation, since the effects of reflection, absorption, eigenmode formation etc. can complicate such estimates. More elaborate modelling [14] provides answers to other questions which are not the main concern of this paper; nevertheless, a comparison with such a model will be made. A direct numerical solution of the equations (4)-(6) for a nonuniform plasma using the initial value problem method is difficult due to the extreme stiffness of the equations associated with presence of an evanescent mode. Moreover, the solution would not simply and conveniently yield the partition of power in various wave modes for the antenna coupling problem. In the following, a uniform plasma model is used, so that the total wave field can be written explicitly as the sum of wave fields of the three different modes. The choices of average density and temperature are made by comparison with an independent computer code [14].

The six constants to be determined for the sixth order system (4)-(6) actually reduce to only three when the appropriate boundary conditions are imposed. These conditions are (a) wave field amplitudes are finite at $\xi = -\infty$ and (b) the energy fluxes are directed towards the negative ξ direction. The wave fields in the plasma may be calculated from the x component of the electric field which is specified in the form:

$$iE_x = \Sigma a_\alpha \exp(-in_\alpha \xi) , \qquad (7)$$

where a_α ($\alpha = B,F,S$) are the three constants to be determined from the coupling condition. The x refractive index n_α is real and negative

for the ion Bernstein wave, since it is a backward propagating wave; it is imaginary and positive for the slow wave, since it is evanescent and finally it is either imaginary and positive or real and positive for the fast wave, depending on whether it is evanescent or propagating, largely determined by the value of n_z. The representation will be seen to satisfy the stated boundary conditions at $\xi = -\infty$. The other components of the electromagnetic field in the plasma ($\xi \leq 0$) may be obtained formally from equations (1)-(7):

$$E_y = -\sum_\alpha \frac{Da_\alpha \exp(-in_\alpha \xi)}{S - n_z^2 - n_\alpha^2} \qquad E_z = -\sum_\alpha \frac{in_\alpha n_z a_\alpha \exp(-in_\alpha \xi)}{P - n_\alpha^2} ,$$

$$cB_x = -n_z E_y , \quad cB_y = -\sum_\alpha \frac{in_z Pa_\alpha \exp(-in_\alpha \xi)}{P - n_\alpha^2} , \quad cB_z = \sum_\alpha \frac{Dn_\alpha a_\alpha \exp(-in_\alpha \xi)}{S - n_z^2 - n_\alpha^2} ,$$

where here and elsewhere, unless otherwise stated the time dependence $\exp(-i\omega t)$ is left implicit.

The formal solution for the electromagnetic field in the vacuum is determined by the boundary conditions at the conducting wall $\xi = \beta$, where $\vec{e}_x \times \vec{E} = 0$ and at the antenna $\xi = \delta$. If $\vec{j}_A(n_z)$ is the Fourier transform of the antenna surface current density, then the jump conditions [...] for the electromagnetic fields across the antenna are

$$\vec{e}_x \times [\vec{E}] = 0 , \qquad \vec{e}_x \times [\vec{B}] = \mu_0 \vec{j}_A(n_z) .$$

The components of the electromagnetic field in the region between the plasma and the antenna are

$$iE_x = -n_z b_z \cos(n\beta - n\xi) + c\mu_0 n_z j_A \cos(n\delta - n\xi) ,$$

$$E_y = b_y \sin(n\beta - n\xi), \quad E_z = -inb_z \sin(n\beta - n\xi) - ic\mu_0 n j_A \sin(n\delta - n\xi) ,$$

$$cB_x = -n_z E_y , \quad cB_y = iE_x/n_z , \quad cB_z = inb_y \cos(n\beta - n\xi) ,$$

where $n^2 \equiv 1 - n_z^2$ and b_y and b_z are the two vacuum constants to be determined from coupling condition. The components in the region between the antenna and the wall may be obtained from the above by setting $j_A = 0$.

An integration of the basic equations (1)-(3) across the plasma-vacuum interface leads to the boundary conditions: $dE_x/d\xi = 0$ at the plasma edge and E_y, E_z, B_y and B_z are continuous across $\xi = 0$. From this follows five matching conditions for the determination of $a_\alpha (\alpha = B,F,S)$, b_y and b_z, which are

$$\sum_\alpha n_\alpha a_\alpha = 0 ,$$

$$\sum_\alpha Da_\alpha/(S - n_z^2 - n_\alpha^2) + b_y \sin n\beta = 0 ,$$

$$\sum_\alpha n_\alpha n_z a_\alpha/(P - n_\alpha^2) - nb_z \sin n\beta = nj \sin n\delta ,$$

$$\sum_\alpha Pn_z a_\alpha/(P - n_\alpha^2) + ib_z \cos n\beta = -ij \cos n\delta ,$$

$$\sum_\alpha Dn_\alpha a_\alpha/(S - n_z^2 - n_\alpha^2) - inb_y \cos n\beta = 0 ,$$

where $j \equiv c\mu_0 j_A$. An elimination of b_y and b_z leads to a simple system of equations for a_α, which in vectorial form is given by

$$\vec{n}.\vec{a} = 0 \ , \quad \vec{X}.\vec{a} = J \ , \quad \vec{Y}.\vec{a} = 0 \ , \tag{8}$$

where the components of $\vec{n}$ and $\vec{a}$ are n_α and a_α and the components of $\vec{X}$ and $\vec{Y}$ are defined by

$$X_\alpha \equiv \frac{n_z(n_\alpha - inPtann\beta)}{P - n_\alpha^2} \ , \qquad Y_\alpha \equiv \frac{D(n - in_\alpha tann\beta)}{S - n_z^2 - n_\alpha^2} \ ,$$

with $J \equiv njsin(n\delta - n\beta)/cosn\beta$. The solution for $\vec{a}$ can be obtained by inspection from (8),

$$\vec{a} = \vec{J}(\vec{n} \times \vec{Y})/\vec{X}.(\vec{n} \times \vec{Y}) \ , \tag{9}$$

where $\vec{X}.(\vec{n} \times \vec{Y}) \neq 0$ from linear independence of the matching conditions. The constants for the vacuum electromagnetic fields are given by

$$b_y = -\frac{J}{cosn\beta}\frac{\vec{U}.(\vec{n} \times \vec{Y})}{\vec{X}.(\vec{n} \times \vec{Y})} \ , \qquad b_z = -j\frac{cosn\delta}{cosn\beta} + \frac{J}{cosn\beta}\frac{\vec{V}.(\vec{n} \times \vec{Y})}{\vec{X}.(\vec{n} \times \vec{Y})} \ ,$$

(10)

where the components of $\vec{U}$ and $\vec{V}$ are defined by

$$U_\alpha \equiv iDn_\alpha/n(S - n_z^2 - n_\alpha^2) \ , \qquad V_\alpha \equiv iPn_z/(P - n_\alpha^2) \ .$$

The antenna-plasma coupling problem has now been formally solved by the expressions (9) and (10), since the electromagnetic fields and energy fluxes at any point in the plasma or in the vacuum may now be evaluated.

In particular, from the above expressions, the component of the electric field at the antenna, parallel to the current is given by

$$E_z = -Z_s(n_z) j_A \ ,$$

where

$$Z_s(n_z) \equiv -i\mu_0 cn \frac{\sin(n\beta - n\delta)}{\cos n\beta} \left\{ \cos n\delta + \frac{n \sin(n\beta - n\delta)}{\cos n\beta} \frac{\vec{V} . (\vec{n} \times \vec{Y})}{\vec{X} . (\vec{n} \times \vec{Y})} \right\} . \quad (11)$$

This will be seen to be the intrinsic spectral impedance of the antenna, since it measures the inherent ability of the antenna to couple power to the plasma as a function of plasma parameters, and positions of the antenna and wall, but it is independent of the shape, size and other spectral characteristics of the antenna.

4. ENERGY FLOW, WAVE POWER PARTITION AND ANTENNA IMPEDANCE

The flow of electromagnetic energy in real space is described by the Poynting flux,

$$\vec{P}(\vec{r}) = \mu_0^{-1} \mathrm{Re}\{\vec{E}^*(\vec{r}) \times \vec{B}(\vec{r})\} ,$$

which has the dimensions of power per unit area (Wm^{-2}). At a given point x, a Poynting vector in k_z Fourier space, which is not a Fourier transform of the above $\vec{P}(\vec{r})$, can be defined independently by

$$\vec{P}(k_z) \equiv \mu_0^{-1} \mathrm{Re}\{\vec{E}^*(k_z) \times \vec{B}(k_z)\} , \tag{12}$$

where $\vec{E}^*(k_z)$ and $\vec{B}(k_z)$ are electromagnetic fields given in the previous section. This Poynting vector $\vec{P}(k_z)$ has the dimensions of power (W) and it is related to $\vec{P}(\vec{r})$ by the following Parseval identity,

$$\int_{-\infty}^{\infty} \vec{P}(\vec{r}) dz = \int_{-\infty}^{\infty} \vec{P}(k_z) dk_z .$$

It is convenient here to use $\vec{P}(k_z)$ rather than $\vec{P}(\vec{r})$.

In a thermal plasma, wave energy can be transported also by collective motion of particles. For electromagnetic fields which vary as $\exp(i\vec{k}.\vec{r}-i\omega t)$, the non-electromagnetic energy flux is given by [15]

$$\vec{T} = -\vec{E}^* \frac{\omega\varepsilon_0}{2} \frac{\partial \overleftrightarrow{K}}{\partial \vec{k}} . \vec{E} ,$$

where $\overleftrightarrow{K}$ is the Hermitian dielectric tensor given by (3). For the variation $\exp(-ik_x x + ik_z z - i\omega t)$ adopted in this paper, this kinetic

energy flux may be written equivalently as

$$\vec{T} = \frac{iT}{\mu_0 c} E_x^* \frac{\partial E_x}{\partial \xi} \vec{e}_x \ , \tag{13}$$

where T is defined in section 2 and $E_x = E_x(k_z)$ is given by (7).

Since the electromagnetic field in the plasma has been partitioned into fields due to the three different wave modes, it is clear that the electromagnetic and kinetic energy fluxes (12) and (13) can be defined individually for each mode, with the corresponding total fluxes defined by

$$<\vec{P}> = \sum_\alpha \vec{P}_\alpha \qquad <\vec{T}> = \sum_\alpha \vec{T}_\alpha \ .$$

In general, at a given point in the plasma, the fluxes due to the total field $\vec{P}$ and $\vec{T}$ differ from the sums of the individual fluxes $<\vec{P}>$ and $<\vec{T}>$ due to correlation energy between different wave modes.

Energy fluxes in the negative x direction associated with the electromagnetic fields of each individual wave mode as well as the total field have been computed for a variety of electron densities and wave numbers. It has been verified that (a) The total energy flux of each individual wave mode is constant (b) $<\vec{P}>$ and $<\vec{T}>$ are respectively the spatial averages as well as the asymptotic values (as $\xi \to \infty$) of $\vec{P}$ and $\vec{T}$, (c) The forward propagating fast waves mainly carry electromagnetic energy whereas the backward propagating ion-Bernstein waves mainly carry kinetic energy associated with the collective motion of ions and (d) Energy conservation in a dissipationless model leads to the following relationship between the intrinsic spectral impedance of the antenna and the wave energy fluxes:

$$\mathrm{Re}(Z_s) j_A^2 = P_x + T_x = \langle P_x \rangle + \langle T_x \rangle = \text{constant}$$

where Z_s is defined by (11).

In antenna-plasma coupling calculations, the properties of the edge region usually have a stronger quantitative effect than those of the central region of the plasma. It is therefore not clear what values one should choose for the average electron density and ion temperature in the uniform model adopted here. In the following, a choice of these parameters is determined from a comparison of the intrinsic spectral impedances calculated, (a) from the uniform model for various combinations of parameters and (b) from a modified version of the computer code developed by Fukuyama et al. [14]. This code, which includes kinetic effects of wave absorption in a nonuniform plasma as well as reflections from boundaries in a geometry essentially the same as that in Fig. 1, was originally developed to study fast wave antenna coupling, where the antenna being orthogonal to the magnetic field couples power mainly to the fast waves. In the modified code, hereafter referred to as FNII*, the alignment of the antenna was altered for slow wave coupling and a single pass solution was obtained by including strong second harmonic cyclotron damping due to a small concentration of extraneous ions. The intrinsic spectral impedance $Z_s(n_z)$ calculated from the uniform model with $n_e = 1 \times 10^{11}$ cm^{-3} and $T_i = 200$ eV is compared in Fig. 2 to points calculated from the FNII* code with parameters and profiles typically those of the JIPP-IIU experiment [11]. It is seen that the agreement between the calculated reactances is excellent and the agreement between the calculated resistances is quite reasonable considering the differences in the physical assumptions used in the models.

For the above choices of average density and temperature and for $n_z = 7.5$, the partition of antenna power into electromagnetic and kinetic energy fluxes is illustrated in Fig. 3. It is seen that under these circumstances, the slow wave antenna very efficiently converts electromagnetic energy flux from the antenna into kinetic energy flux in the plasma. Moreover, the total energy flux is carried almost exclusively by ion Bernstein waves in the plasma, since at such low densities and at relatively large k_z, the fast waves are evanescent. At higher densities however fast waves can propagate and thus carry power away from the antenna, as illustrated e.g. in Fig. 4 for a case where $n_o = 1 \times 10^{13}$ cm^{-3}; nevertheless, for reasonable values of the average density, the fraction of antenna power going into fast waves is small.

To estimate the actual impedance of the type III antenna in the JIPP T-IIU experiment [11], consider a surface current density at the antenna $\xi = 0$ given by

$$\vec{j}_A(z) = \frac{\pi I}{4 l_y} \cos\left(\frac{\pi z}{2 l_z}\right) H(z, l_z) \vec{e}_z \ , \tag{14}$$

where l_y and l_z are respectively the half widths of the antenna in the y and z directions, I is the average antenna current, and $H(z,l_z)$ is the Heavyside step function for $-l_z \leq z \leq l_z$. The current density distribution has been chosen so that the integral of $\nabla.\vec{j}_A$ vanishes and hence there is no charge accumulation at the antenna. This avoids the consideration of current feeders [16] which complicates the estimate by introducing a new dimension to the problem. The Fourier transform of the antenna current distribution (14) is given by

$$\vec{j}_A(k_z) = -(\pi I l_z/8 l_y) S(k_z) \vec{e}_z \ ,$$

where the antenna spectral function is defined by

$$S(k_z) = \cos(k_z l_z)/(k_z^2 l_z^2 - \pi^2/4) \ .$$

The complex impedance of the antenna Z is related to the complex power P dissipated at the antenna by the definition

$$P = \frac{1}{2} Z I^2 \ .$$

From the above expressions and those in section 3,

$$P = -\frac{1}{2} \int_{-\infty}^{\infty} F(k_z) Z_s(k_z) dk_z \ , \qquad (15)$$

where we have introduced an antenna spectral form factor by $F(k_z) \equiv (\pi^2 l_z^2/32 l_y) S^2(k_z)$. This form factor depends only on antenna geometry and its current distribution and it is independent of the coupling conditions to the plasma. The form factor is therefore a weighting function which determines the relative contributions of various ranges of k_z in $Z_s(k_z)$ to the actual antenna input impedance. This is graphed for $2 l_y = 0.2\text{m}$ and for various l_z in Fig. 5, where the expected trend of broader spectrum for smaller l_z is observed. The corresponding antenna input impedances have been evaluated from (15) and tabulated in Table I, for the reference case where $n_e = 1 \times 10^{11}\ \text{cm}^{-3}$ and $T_i = 200\,\text{eV}$. It is seen that in this case, the input impedance is largest when the antenna length is about 0.2m.

However, energy deposition profiles calculated from the FNII* code show edge heating due to electron Landau damping when $n_z > 20$. Hence it is important to balance the advantages of smaller antenna lengths in the z direction with sufficient power penetration into the plasma.

The input impedance of the type III antenna used in JIPP T-IIU experiments ($l_y = 0.1m$, $l_z = 0.25m$) had been calculated from (15) for a number of average ion temperatures and a range of average densities. It is seen that the antenna resistance tends to increase with temperature but decrease with density, whereas the input reactance is relatively insensitive to temperature variations, but tends to increase with density.

TABLE I. ANTENNA IMPUT IMPEDANCES

Antenna Length	Resistance	Reactance	Quality Factor
$2l_z$ (metres)	R(ohms)	X(ohms)	Q = X/R
0.1	0.37	150	410
0.2	0.55	170	310
0.3	0.45	120	270
0.4	0.35	94	270
0.5	0.28.	76	270
0.6	0.22	63	290
0.7	0.18	53	290

5. SUMMARY AND DISCUSSIONS

A slow wave antenna has been shown theoretically to be highly efficient in launching ion Bernstein waves directly; the fraction of antenna power going into fast waves is generally very small. These conclusions are consistent with independent computer calculations using the FNII* code [14]. The results show that efficient antenna coupling to ion Bernstein waves can occur under wide ranges of densities and temperatures and it does not depend on special circumstances such as the existence of a confluence in the dispersion curves of the plasma. It appears from equation (4) that a strongly evanescent slow wave drives the perpendicular electric field of an ion Bernstein wave by classical electromagnetic coupling. It is hoped that these results will be useful in interpreting the experimental observations obtained from a number of machines [9-11]. In particular, the large increases in perpendicular ion temperature observed recently [18] in the JIPP T-IIU tokamak during ICRF heating can be explained by the efficient slow wave antenna coupling to ion Bernstein waves, which carry mainly perpendicular kinetic energy associated with the collective motion of ions.

It is evident from the present investigation that ICRF heating using slow wave coupling has a number of advantages and disadvantages compared to conventional ICRF heating using fast wave coupling. It has been pointed out [7], the dimension along the direction of the magnetic field of the coupling structure is much smaller for slow wave coupling than for fast wave coupling. The possibility exists, for example, for a simple waveguide RF coupler to be fitted into the space between toroidal field coils in a reactor tokamak. The present study shows that to avoid excessive surface

heating due to electron Landau damping, the z-dimension of the coupling structure should still exceed about 20 cm. The large kinetic energy flux at the edge of the plasma observed in the present calculation indicates that surface heating due to ion-ion collisions in the cooler edge region might be important and therefore should be assessed. However, both the efficientcy of slow wave coupling and the avoidance of surface heating are expected to improve in hotter plasmas of the future. Moreover, slow wave coupling is largely insensitive to the relative concentrations of the ionic mixtures, particularly when compared to fast wave coupling from the low field side of a tokamak. On the other hand, slow wave coupling usually leads to higher antenna Q factors and hence results in higher antenna voltages for a given antenna current; this tends to limit the total power a given coupler can deliver to the plasma.

Finally, it should be mentioned that the presence of magnetic shear and a poloidal magnetic field may affect the branching ratio between fast waves and ion Bernstein waves and therefore should be investigated.

ACKNOWLEDGEMENTS

One of us (W.N-C. Sy) wishes to thank the Japanese Society for Promotion in Science for financial support and the Institute of Plasma Physics for kind hospitality during his visit to Nagoya. Another author (T. Watari) thanks Dr. Ono of PPPL for valuable discussions.

REFERENCES

[1] JACQUINOT, J., McVEY, B.D., SHARER, J.E. Phys. Rev. Lett. 39 (1977) 88.

[2] SWANSON, D.G., NGAN, Y.C., Phys. Rev. Lett. 35 (1975) 517; CHIU, S.C., MAU, T.K., Nucl. Fusion 23 (1983) 1613.

[3] EQUIPE TFR, Plasma Phys. 24 (1982) 615.

[4] HWANG, D., BITTER, M., BUDNY, R., CAVALLO, A., CHRIEN, R., et al., in Plasma Physics and Controlled Nuclear Fusion Research (Proc. 9th Int. Conf. Baltimore, 1982) Vol. 2, IAEA Vienna (1983) 3.

[5] KIMURA, H., MATSUMOTO, H., ODAJIMA, K., KONOSHIMA, S., SUZUKI, N., et al., ibid, 113; ICHIMURA, M., FUJITA, J., HIROKURA, S., KAKO, E., KAWAHATA, K., et al., Nucl. Fusion (1984).

[6] PURI, S., Phys. Fluids 22 (1979) 1716.

[7] ONO, M., STIX, T.H., WONG, K.L., HORTON, R., in Proceedings of the Second Joint Grenoble-Varenna International Symposium on Heating in Toroidal Plasmas (Commission of the European Communities, Brussels, 1980), Vol. 1, p. 593.

[8] ONO, M., WURDEN, G.A., WONG, K.L., Phys. Rev. Lett. 52 (1984) 37.

[9] WATARI, T., ADATI, K., AOKI, T., HIDEKUMA, S., HATTORI, K. et al., Nucl. Fusion 22 (1982) 1359.

[10] SHOJI, T., TSUBOI, F., TAKASUGI, K., WHANG, K., KISHIMOTO, S., et al., in Proceedings of the Fourth Joint Grenoble-Varenna International Symposium on Heating in Toroidal Plasmas (Commission of the European Communities, Brussels, 1984), Vol. 1, p. 413.

[11] WATARI, T., ONO, M., ANDO, R., FUJITA, J., HIROKURA, Y., et al., ibid, Vol. 1, p. 419 (also in IPPJ-662).

[12] HASEGAWA, A., Phys. Fluids 8 (1965) 761.

[13] SY, W.N-C., COTSAFTIS, M., Plasma Phys. 21 (1979) 985.

[14] FUKUYAMA, A., NISHIYAMA, S., ITOH, K., ITOH, S.-I., Nucl. Fusion, 23 (1983) 1005.

[15] STIX, T.H., The Theory of Plasma Waves, McGraw-Hill, New York (1962), p. 10, and p. 50.

[16] BHATNAGAR, V.P., KOCH, R., MESSIAEN, A.M., WEYNANTS, R.R., Nucl. Fusion 22 (1982) 280.

[17] EVRARD, M.P., WEYNANTS, R.R., in Proceedings of the Third Joint Grenoble-Varenna International Symposium on Heating in Toroidal Plasmas (Commission of the European Communities, Brussels, 1982), Vol. 1, p. 375.

[18] TOI, K., WATARI, T., OHKUBO, K., KAWAHATA, K., NODA, N., et al., in Plasma Physics and Controlled Nuclear Fusion Research (Proc. 10th Int. Conf. London, 1984) Paper IAEA-CN-44/F-III-2.

FIGURE CAPTIONS

Fig. 1. Geometry of the model and dispersion curves for typical JIPP T-IIU parameters: $n_e \cong 2.25 \times 10^{13}$ cm^{-3}, $T_i \cong 300$ eV, $B_\phi = 1.8$T (on axis values) and at 40 MHz. The x refractive indices squared for ion Bernstein waves, fast waves and slow waves are denoted respectively by n_B^2, n_F^2, n_S^2.

Fig. 2. The intrinsic spectral impedance vs z refractive index calculated from the uniform model with $n_e = 1 \times 10^{11}$ cm^{-3}, $T_i = 200$ eV, $B_\phi = 1.5$T, at 40 MHz. The points are obtained from the FNII* code [14] using the parameters of Fig. 1.

Fig. 3. Partition of Antenna power into electromagnetic and kinetic components: (a) T_x, (b) $\langle T_x \rangle$, (c) P_x and (d) $\langle P_x \rangle$ for the parameters of Fig. 2 with $n_z = 7.5$.

Fig. 4. Partition of antenna power into ion Bernstein waves and fast waves at high density $n_e = 1 \times 10^{13}$ cm^{-3}.

Fig. 5. Antenna spectral form factor for $l_y = 0.1$m and for various values of l_z, the antenna length along the magnetic field.

Fig. 6. Estimated input impedance of the type III antenna used in the JIPP T-IIU experiments [11] calculated from the uniform model for various temperatures and a range of densities: (a) resistance and (b) reactance.

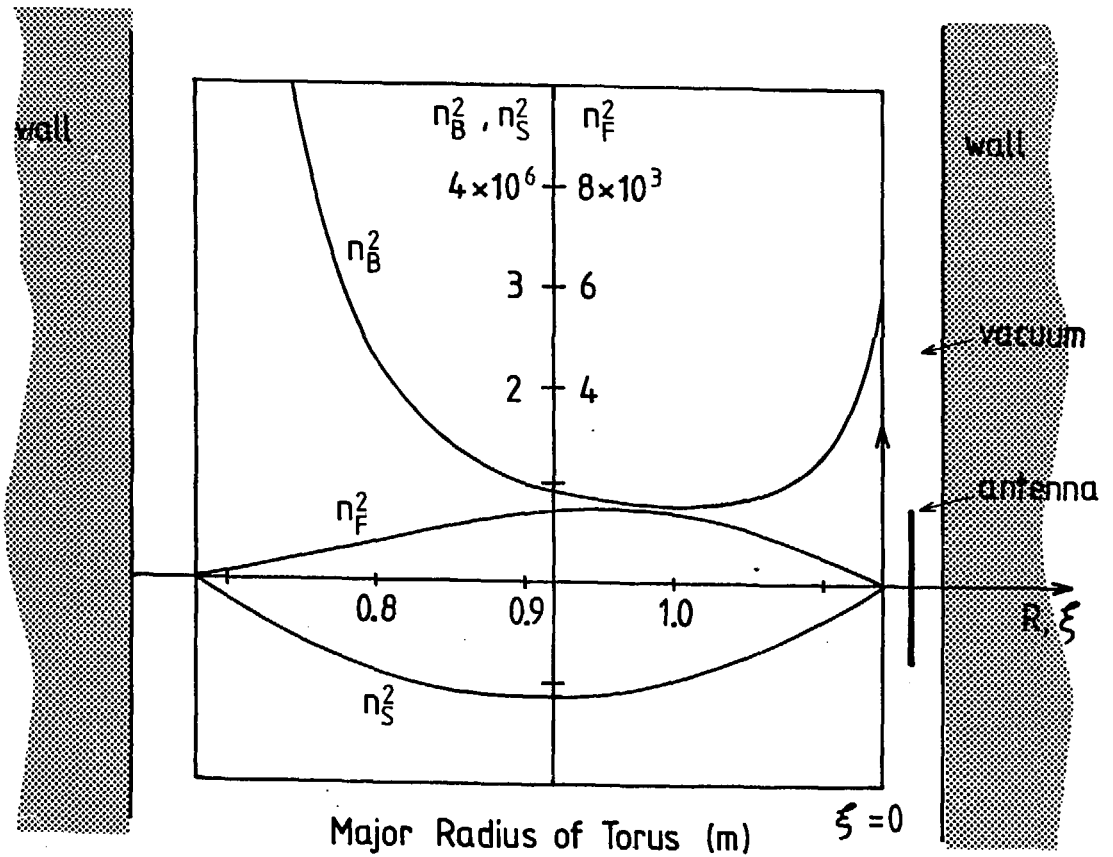
wall
wall
n_B^2 , n_S^2
n_F^2
4×10^6
8×10^3
n_B^2
3
6
2
4
vacuum
antenna
n_F^2
0.8
0.9
1.0
R, ξ
n_S^2
Major Radius of Torus (m)
ξ =0

fig.1

fig. 2

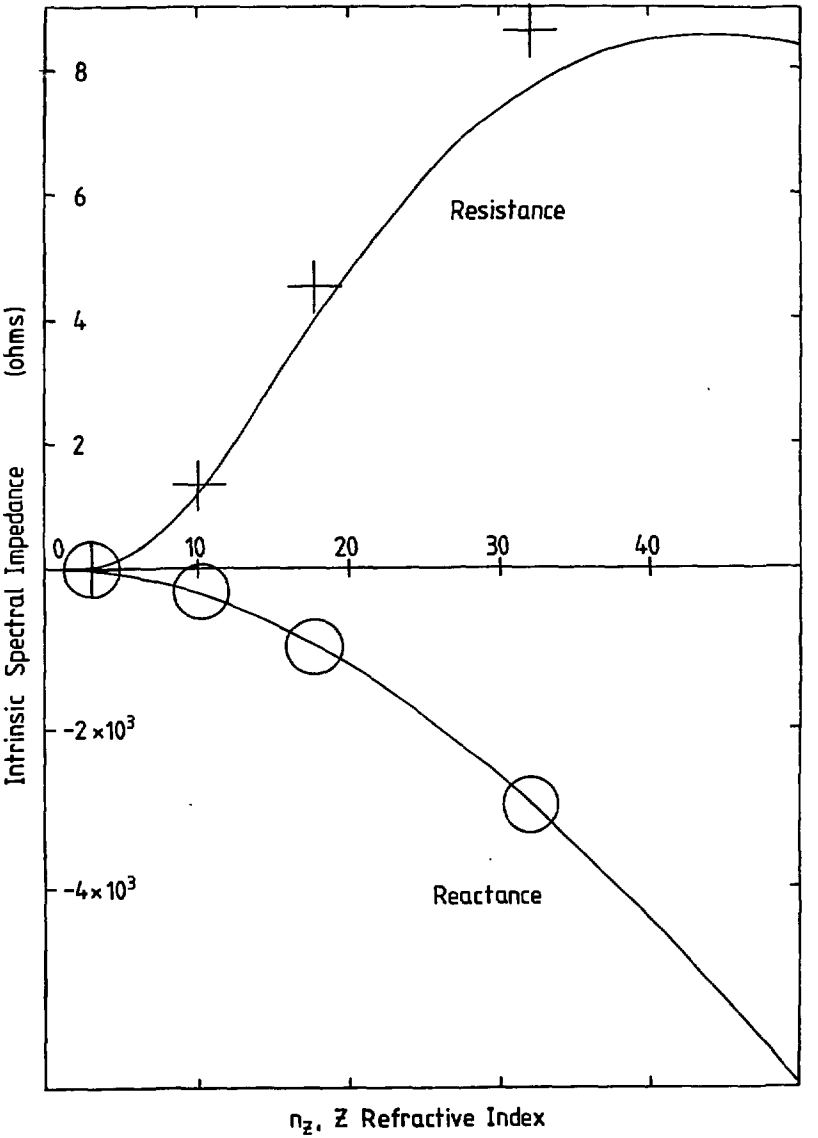
8
6
4
2
0
10
20
30
40
Resistance
Reactance
-2×10³
-4×10³
Intrinsic Spectral Impedance (ohms)
n_z, Ż Refractive Index

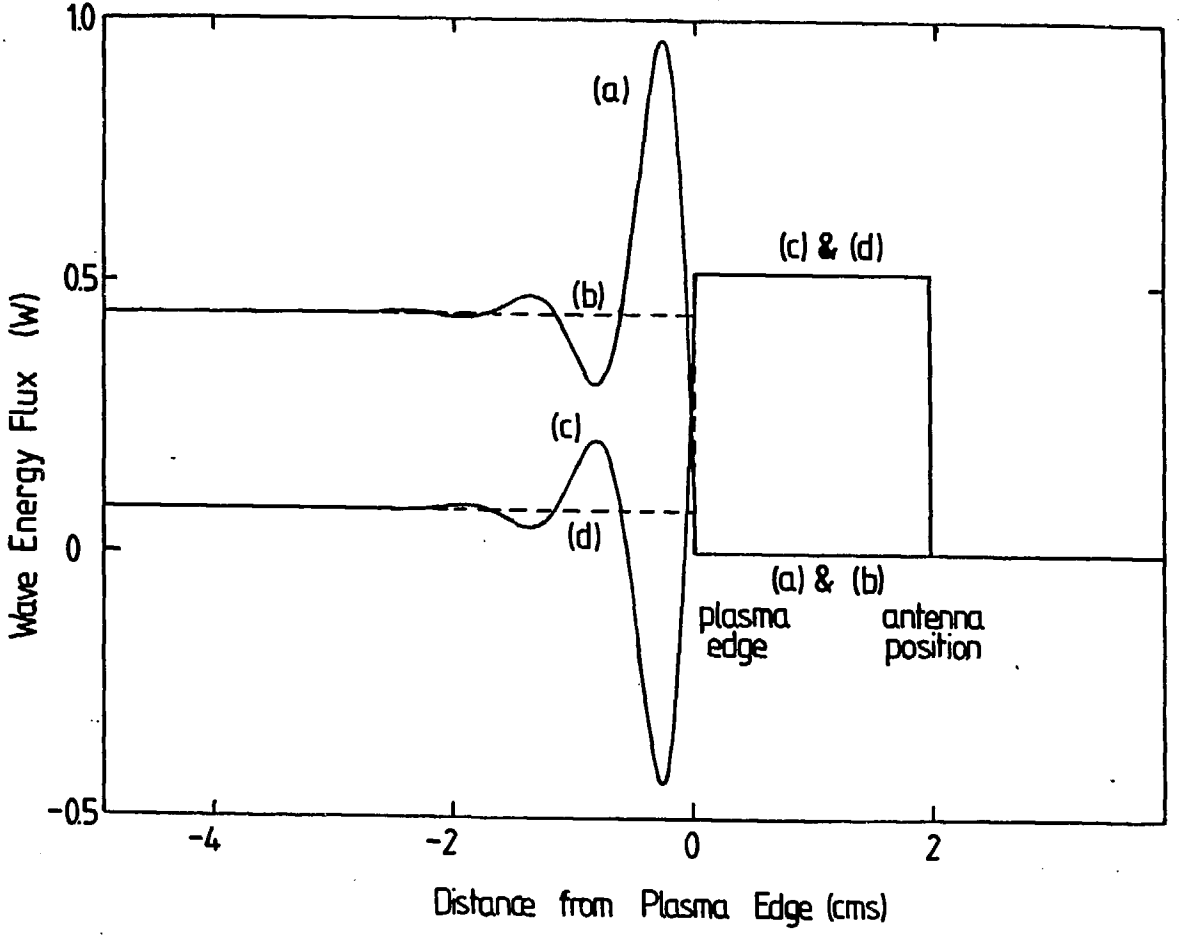
1.0
0.5
0
-0.5
Wave Energy Flux (W)
(a)
(b)
(c)
(d)
(c) & (d)
(a) & (b)
plasma edge
antenna position
-4
-2
0
2
Distance from Plasma Edge (cms)

fig. 3

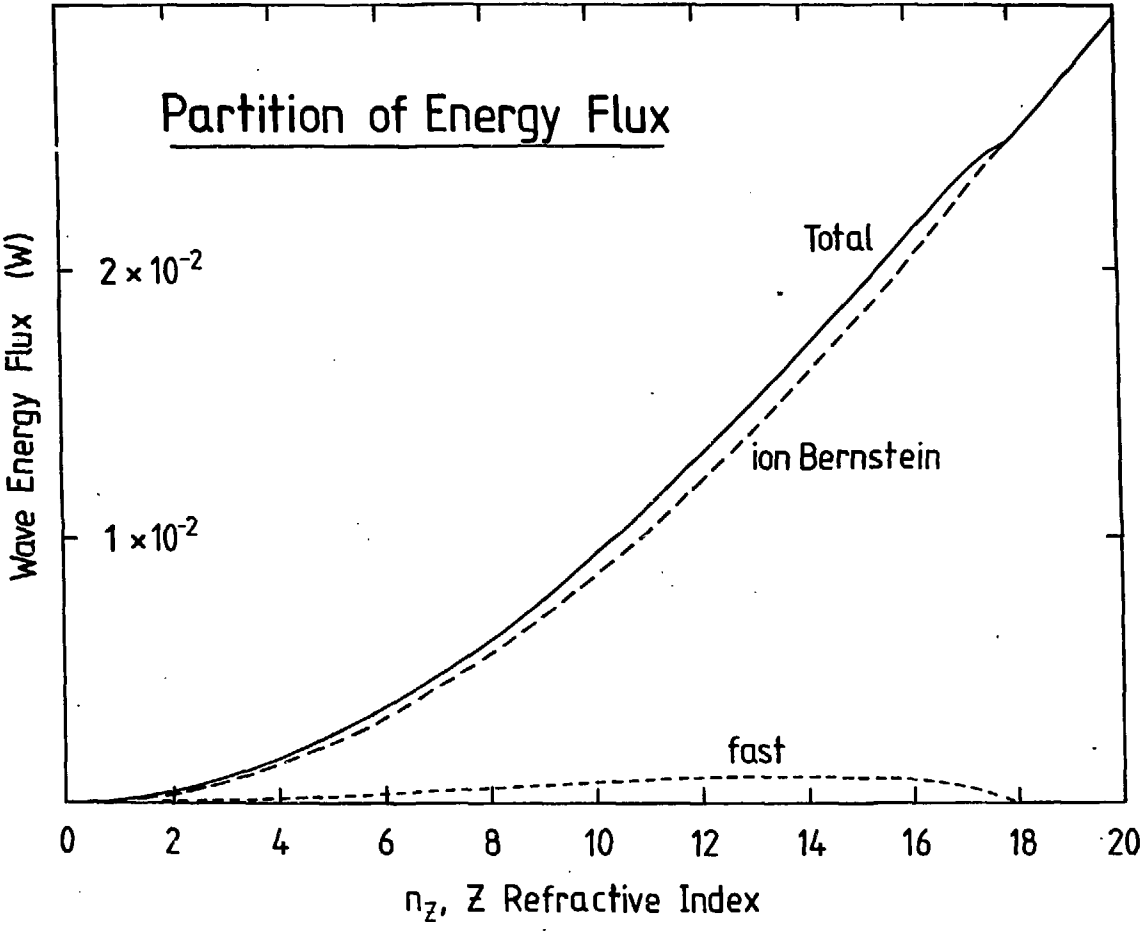
Partition of Energy Flux
Wave Energy Flux (W)
2 × 10⁻²
1 × 10⁻²
Total
ion Bernstein
fast
0
2
4
6
8
10
12
14
16
18
20
n_Z, Z Refractive Index

fig. 4

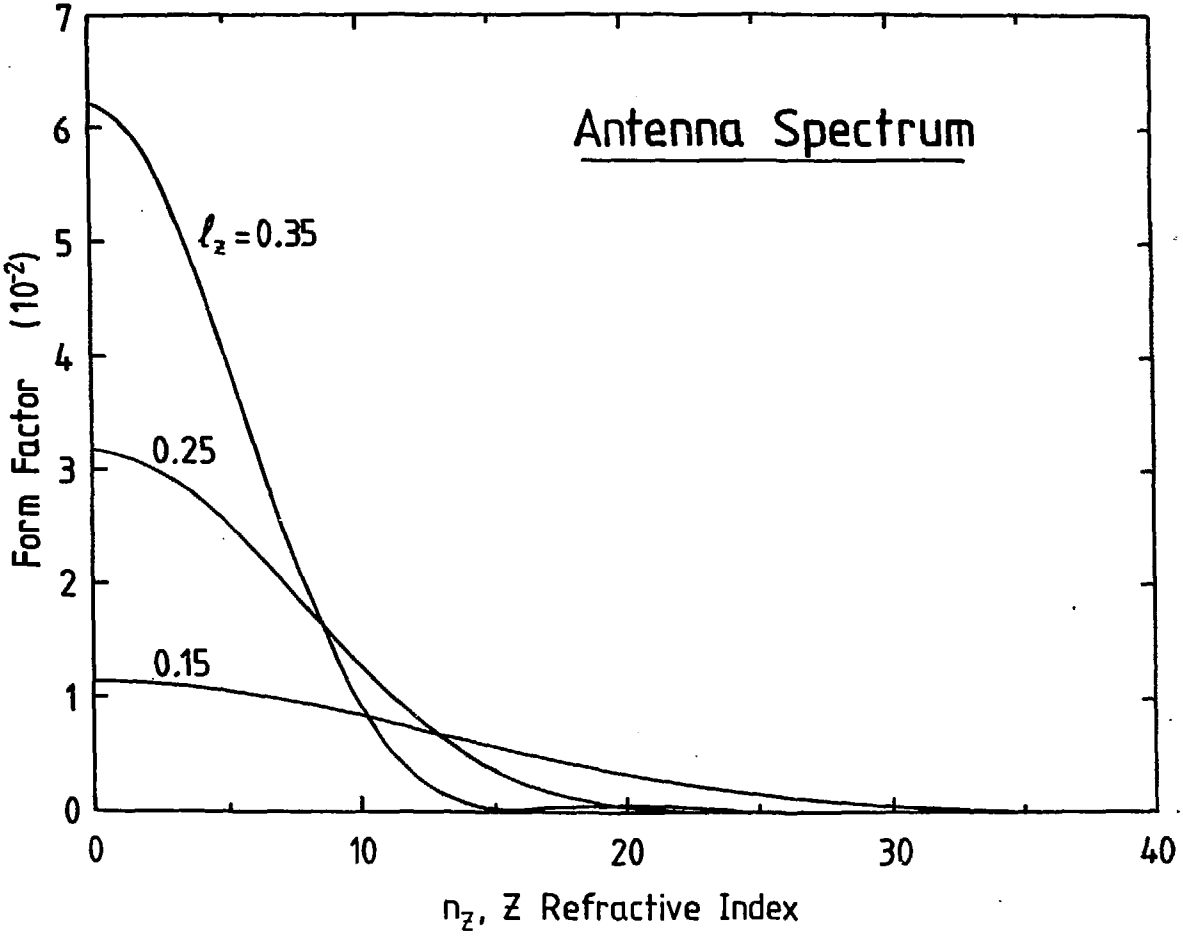
Antenna Spectrum
$\ell_z = 0.35$
0.25
0.15
Form Factor (10^{-2})
n_z, Z Refractive Index
0
1
2
3
4
5
6
7
0
10
20
30
40

fig. 5

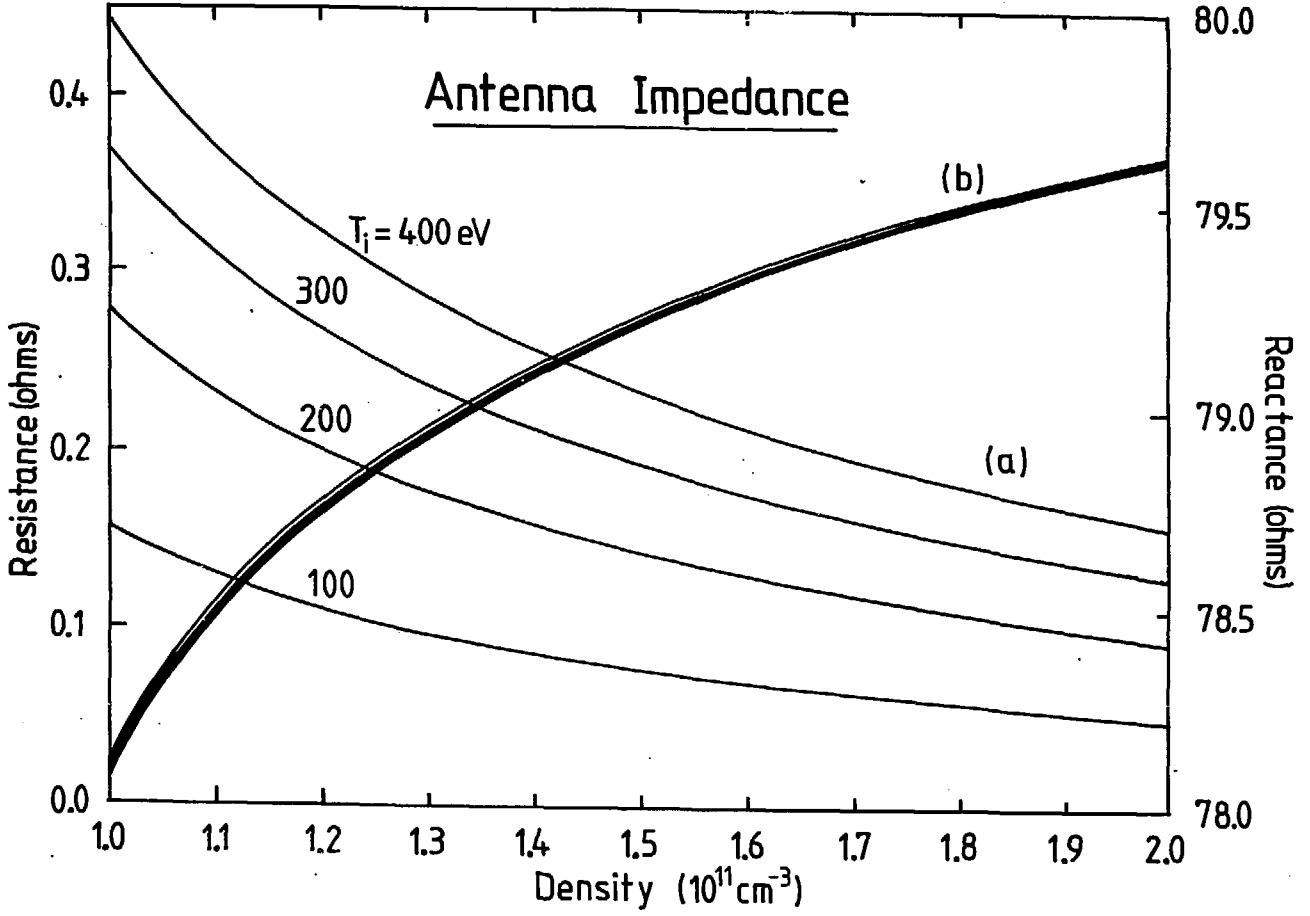
Antenna Impedance
(b)
T_i = 400 eV
300
200
100
(a)
Resistance (ohms)
Reactance (ohms)
0.0
0.1
0.2
0.3
0.4
78.0
78.5
79.0
79.5
80.0
1.0
1.1
1.2
1.3
1.4
1.5
1.6
1.7
1.8
1.9
2.0
Density (10^{11} cm^{-3})

fig. 6